Telecommun Syst (2012) 50:297–309
DOI 10.1007/s11235-010-9405-0

The multi-copy diversity for routing in sparse vehicular ad hoc networks

Joon Yoo · Sunwoong Choi · Chong-kwon Kim

Published online: 9 December 2010

Abstract The need for routing based on store-and-carry forwarding has been motivated in sparse vehicular ad hoc networks (VANETs), since the traditional end-to-end unicast routing is infeasible due to the network disconnection problem. In store-and-carry based routing, the end-to-end message delivery delay is dominated by the store-and-carry procedure rather than the wireless transmission. Therefore, the end-to-end delay in such sparse VANETs can be further reduced by replicating multiple copies of the message to other nodes when possible, i.e., multi-copy routing, to increase the chance of finally finding the destination, which we call this gain as *multi-copy diversity*. In this paper, we present an analytic framework to evaluate the performance of routing by assessing the multi-copy diversity gain in sparse VANETs. By using this model, we first derive an upper and lower-bound of end-to-end routing delay in sparse VANETs. Our analytic results show that a high level of multi-copy diversity gain is achieved when the network is *partially* connected, which is in contrast to the conventional expectation that multi-copy routing performs better in severely disconnected networks. Second, we propose a new adaptive multi-copy VANET routing scheme called AMR by exploiting these analytic results. AMR adapts to the local network connectivity and increases the level of multi-copy diversity at significantly reduced routing overhead compared to the well known epidemic routing. We validate the accuracy of our analytic model and the performance of AMR via simulation studies.

Keywords Vehicular networks · Multi-copy diversity · Store-and-carry forwarding · Delay bound · Performance modeling

1 Introduction

Recently advanced technology of vehicular networks is envisioned to become a common platform to support a plethora of intelligent transportation applications that improve safety, convenience, and comfort of everyday road travel. Safety applications have drawn much attention in the automotive industry since it provides advanced accident prevention by generally employing impromptu broadcast communications. Informative applications, such as sending queries to point of interest via multi-hop communications, usually employ unicast transmissions. In this paper, we focus on the second class of informative unicast applications.

In *sparse* vehicular ad hoc networks (VANETs), traditional unicast routing is not directly feasible since the unicast routing path is usually disconnected due to the intermittent nature of network links. VANETs at low densities may get disconnected due to low node density at the time of day such as night times or low deployment rate at market introduction phase [2, 5, 6, 10, 14, 15]. As a result, a mobile node can be used as a carrier to deliver messages, i.e., *store-and-carry forwarding* which is a technique developed by the delay tolerant network (DTN) community [1, 11].

J. Yoo (✉)
Computer Science Department, UCLA, 420 Westwood Plaza, Los Angeles, CA, 90095, USA
e-mail: joonyoo2@ucla.edu

S. Choi
School of Electrical Engineering, Kookmin University, Seoul 136-702, Republic of Korea

C.-k. Kim
School of Electrical Engineering and Computer Science, Seoul National University, Seoul 151-742, Republic of Korea

Epidemic routing [13] is a representative example that employs store-and-carry forwarding, where a node receiving a packet stores and carries, and passes the packet whenever it meets a new encountering node which does not have a copy of the packet. The node keeps passing the packet until it finally meets the destination. By replicating multiple copies of the same packet, it increases the chance to find the destination, thus reduces the delay, while trading off network resources such as bandwidth and storage. We refer to this phenomenon as *multi-copy diversity* gain, and the multi-copy diversity effect on DTNs with random mobility is evaluated in [16]. Epidemic routing, with some improvements, has recently been applied to the vehicular networks to combat the network disconnection problem [2, 5, 6, 10, 15]. The main difference of epidemic routing in vehicular networks is that the packet replication is only made at the *intersection*, where multiple available road paths to the destination may exist. At the road sections (the straight roads where there is no alternative paths), the packet is only greedily forwarded to the next intersection that leads to the path towards the destination.

One major challenge of modeling routing performance based on store-and-carry forwarding in sparse networks is the mobility of nodes. In traditional DTNs, it is assumed that the *meeting rate* between nodes is nearly exponential with random node mobility, such as random waypoint or random walk [16]. Accordingly, the performance of epidemic routing is evaluated by deriving the probability distribution of end-to-end delay employing the exponential meeting rate [5]. However, the meeting rate between nodes is no longer the main factor that affects routing performance in sparse VANETs since *location-based routing* with the road map information is typically deployed [5, 7, 8]. The digital road map topology as well as the geographical location of the vehicle itself and the destination can be easily acquired via global positioning system (GPS) devices and location servers [17]. Based on this knowledge, all the vehicles in the network can calculate the potential routing road paths to the destination. Therefore the main factor that affects the routing performance is the achievable multi-copy diversity at the intersections rather than the node meeting-rate as in general DTNs.

In this paper, we develop an analytical framework to study the performance of store-and-carry routing in sparse VANETs. In particular, we evaluate the multi-copy diversity by modeling the vehicular distribution at the road sections and intersections. In result, we obtain an upper-bound and lower-bound of end-to-end routing delay that uses multi-copy routing. The numerical results show that multi-copy routing achieves a large multi-copy diversity gain over single-copy routing when the network is partially connected. This is in stark contrast to the expectation that multi-copy routing achieves better performance gain when the network is mostly disconnected. Furthermore, we propose a heuristic Adaptive Multi-copy Routing protocol called AMR. AMR exploits our analytic results by adapting to the local network connectivity. We show that AMR achieves multi-copy diversity close to maximum while limiting the routing overhead. AMR also utilizes only the *local* delay measurements, while previous sparse routing protocols [2, 10, 15] requires *global* network information at real time.

In summary, we make three key contributions in this paper. First we develop a framework for modeling the routing performance in sparse vehicular networks. Our framework exploits multi-copy diversity to evaluate the end-to-end routing delay bound. Second, we propose an adaptive multi-copy routing protocol. AMR leverages the close to maximum multi-copy diversity with limited overhead. Finally, we conduct extensive simulations first to validate the accuracy of our analytic model, and second to show the performance of AMR that achieves end-to-end delay comparable to that of epidemic routing while significantly reducing the routing overhead by up to 86%.

The remainder of the paper is structured as follows. In Sect. 2 we lay out the related work. Section 3 presents the multi-copy diversity effect via analytical modeling of the vehicular distribution at the road sections and intersections, and Sect. 4 provides an upper-bound and lower-bound of end-to-end routing delay in sparse vehicular networks. Section 5 gives detailed description of the AMR protocol and Sect. 6 evaluates the performance of AMR via simulations. Finally, Sect. 7 concludes this paper.

2 Related work

Many routing protocols have been proposed to deal with the disconnection problem in sparse vehicular networks [2, 5, 6, 10, 15]. Vehicle-Assisted Data Delivery (VADD) [15] uses global statistical traffic information, such as vehicle speed and density to measure the expected delay at each road, and in result, finds the path with the lowest expected end-to-end delay. Delay-bounded routing [10] uses a similar approach but attempts to adhere delay constraints induced by applications. The aforementioned approaches assumed that real-time *global* traffic information of the area, which may extend up to tens or even hundreds of square miles depending on the location of the destination, is known to the vehicles a priori, which may not be practical. Static-node assisted Adaptive data Dissemination (SADV) [2] improves VADD with the assistance of static nodes at intersections. The static node assists the vehicles by storing a message until a vehicle appears along the best delivery path to reduce the end-to-end delay, and also measures the delay between adjacent static nodes at real time. Trajectory-Based Data Forwarding (TBD) [6] enhances VADD by exploiting

the vehicle's trajectory information in routing. In Shanghai urban vehicular network (SUVnet) [5], a message is copied only to the vehicles that are both located nearer and moving towards the destination to reduce the overhead of epidemic routing. These studies focus on proposing and evaluating protocols only through simulations, while we propose an analytical framework to measure the routing performance in sparse VANETs.

Several analytic mobility models for VANETs have been proposed [9, 14]. Mohimani et al. [9] model VANET mobility by employing an open queueing network comprising M/G/∞ nodes. Wisitpongphan et al. [14] propose an analytical model based on realistic traffic traces to evaluate the routing performance of vehicular networks at highways. But since the analysis concentrates on approximation through mean value studies, the re-healing time results shows some inaccuracies, while our model derives the probability distribution to acquire the relatively accurate delay bound of multi-copy routing.

In recent years, routing in DTN has been extensively studied. Epidemic routing [13] has been proposed for routing in general mobile networks with random mobility, in which case the inter-meeting time is nearly exponentially distributed [16]. In vehicular ad hoc networks, the exponential meeting time assumption should only hold for specific cases such as DieselNet [1], which is a network of buses that travels on predetermined routes, and is not well suited for general vehicular networks. Furthermore, geographical location information of the vehicles including the destination can be easily acquired via GPS devices or location servers [17]. Therefore, as mentioned before, as we may use geographical routing [7], i.e., know all the potential paths to the destination via location information, the critical factor that determines the end-to-end delay is the probability distribution of delay at each road sections and intersections rather than inter-meeting time distribution.

Spyropoulos et al. [11] propose a multi-copy routing scheme to reduce the overhead of epidemic routing by restricting the number of message copies to L. To choose the minimum L value that meets the specific delay constraint, the global network information such as the number of nodes is required. Our approach in AMR uses a similar approach by restricting the number of messages while maintaining the end-to-end delay close to that of epidemic routing.

3 Multi-copy diversity analysis in sparse VANETs

The end-to-end delay of location-based routing consists of the sum of the delays at the end-to-end routing path, which consists of road sections and intersections. For example, as shown in Fig. 1, the end-to-end packet delay between node A and B is equal to the sum of the packet delays at the roads and intersections that are a part of the potential path from node A to B. The routing delay performance depends on the multi-copy diversity made at each intersection. In other words, if the message is copied to multiple roads at the intersection, then the routing delay typically decreases. Therefore, we model the probability distribution of message delivery delay at each road sections and intersections. We first present the system model of a vehicular ad hoc network, which consists of road sections and intersections, in Sect. 3.1. We then model a one-way road section to derive the probability distribution of delay and in result evaluate the multi-copy diversity for routing in Sect. 3.2. We finally analyze the intersection model in Sect. 3.3.

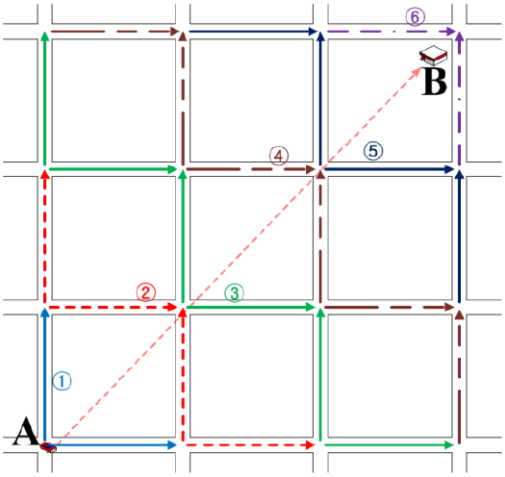

Fig. 1 Multi-copy routing stages in a vehicular network. Source node A sends a message towards destination node B

3.1 System model

In this subsection, we describe the system model used in our analysis to develop an analytical model to evaluate the routing performance of sparse VANETs. A VANET system consists of road sections (Sect. 3.2) and intersections (Sect. 3.3), as illustrated in Fig. 2. L (m) denotes the length of a one-way road section, which is equivalent to the distance between two adjacent intersections. Let λ (veh/m) denote the average vehicle density which corresponds to the number of vehicles per unit distance along the road section. R_{TX} (m) denotes the wireless transmission range of the radio transmitter on a vehicle, and v_{avg} (m/s) denotes the average moving speed of a vehicle. Since we consider only sparse networks, the vehicle speed does not depend on the preceding vehicle, as in the car following model [4], but rather on the speed limit of the road. Thus, we assume that vehicles travel at a constant speed of v_{avg} on each road, which is consistent with [2, 6] and [14]. Therefore, if a vehicle does not exist within the transmission range at the message-forwarding direction, then the message has to be stored-and-carried until it reaches

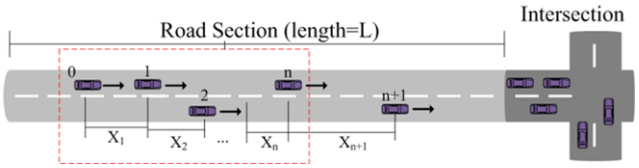

Fig. 2 Network model of a road section and intersection

the next intersection, which should be more crowded than the road section due to traffic lights or stop signs [3, 4]. The intersection model is presented in Sect. 3.3.

The inter-vehicle distance between vehicle i and the next vehicle in front of vehicle i, vehicle $i+1$, is represented as a random variable X_i. According to the measurement results in [14] and realistic mobility model in [12], the inter-vehicle distance follows a nearly exponential distribution especially when the vehicles are sparsely distributed in both city [12] and highway [14] scenarios. Therefore we assume that X_i is independent and identically distributed (i.i.d.) and exponentially distributed following the exponential *probability density function* (PDF) of $\lambda e^{-\lambda x}$. Since the delay for wireless transmissions is in the order of *milliseconds* while the delay for carry-and-forward is in the order of *tens of seconds*, we assume that the wireless transmission delay ≈ 0 [2, 6, 15]. For the sake of simplicity in our analysis, we assume that all roads are homogeneous so that parameters such as wireless transmission range, road length, average density, and average vehicle speed are the same for each road in the network. Notice that this can be easily extended to non-homogeneous environments with some added notations. Finally, we denote the probability of a vehicle existing within the transmission range as

$$\Pr(X_i \le R_{TX}) = 1 - e^{-\lambda R_{TX}} \equiv p, \quad \forall i > 0 \tag{1}$$

3.2 One-way road section analysis

In this subsection, we first develop an analytical model to derive the probability distribution of delay in a one-way road section[1] and then study the multi-copy diversity gain at the intersection by evaluating expected delay when k path choices are available. As shown in Fig. 2, vehicles form a cluster at the start of a road section. Let random variables C and N denote the cluster length and the number of vehicles in a cluster, respectively. To form a cluster with length C and N vehicles, there should be $(N-1)$ consecutive vehicles that have a vehicle within transmission range in front and *no* vehicle within transmission range in front of the N-th vehicle. Therefore, the probability distribution of cluster length C is

$$\begin{aligned}\Pr(C \le x) &= \sum_{n=1}^{\infty} \Pr(N=n) \cdot \Pr(C \le x | N=n) \\ &= \Pr(N=1) \cdot \Pr(C \le x | N=1) \\ &\quad + \sum_{n=2}^{\infty} \Pr(N=n) \cdot \Pr(C \le x | N=n) \\ &= (1-p)\Bigg(1 + \sum_{n=1}^{\infty} p^n \cdot \Pr(X_1 + X_2 + \cdots \\ &\quad + X_n \le x | \forall X_i \le R_{TX}, i = 1, \ldots, n)\Bigg)\end{aligned} \tag{2}$$

Next we derive the rightmost probability in the last part of (2). Since X_i has to be smaller than R_{TX}, the *cumulative distribution function* (CDF) and PDF of X_i is given by,

$$\begin{aligned} F_{X_i|R_{TX}}(x) &= \Pr(X_i \le x | X_i \le R_{TX}) = \frac{1 - e^{-\lambda x}}{p} \\ f_{X_i|R_{TX}}(x) &= \frac{\lambda}{p} e^{-\lambda x} \end{aligned} \tag{3}$$

respectively, where $0 \le x \le R_{TX}$. Since the n random variables of X_i's are independently distributed, the probability distribution of a cluster is given by n convolutions of $f_{X_i|R_{TX}}(x)$, which we denote as $f^{n*}_{X_i|R_{TX}}(x)$. Therefore, (2) can be reformulated as,

$$\begin{aligned}\Pr(C \le x) &= (1-p)\Bigg(1 + \sum_{n=1}^{\infty} p^n \cdot \int_0^x f^{n*}_{X_i|R_{TX}}(t)dt\Bigg) \\ &= (1-p)\Bigg(1 + \int_0^x \sum_{n=1}^{\infty} p^n \cdot f^{n*}_{X_i|R_{TX}}(t)dt\Bigg) \\ &= (1-p)\Bigg(1 + \int_0^x h(t)dt\Bigg)\end{aligned} \tag{4}$$

where $h(t) = \sum_{n=1}^{\infty} p^n \cdot f^{n*}_{X_i|R_{TX}}(t)$. Now, we obtain $F(s)$ which is the Laplace transform of $f_{X_i|R_{TX}}(x)$.

$$F(s) = \int_0^{\infty} e^{-st} f_{X_i|R_{TX}}(t)dt = \frac{\lambda}{p} \cdot \frac{1 - e^{-(s+\lambda)R_{TX}}}{s+\lambda} \tag{5}$$

Using this result, we obtain $H(s)$, which is the Laplace transform of $h(t)$.

$$\begin{aligned} H(s) &= \sum_{n=1}^{\infty} p^n \cdot F^n(s) = \frac{pF(s)}{1 - pF(s)} = \frac{\lambda(1 - e^{-(s+\lambda)R_{TX}})}{s + \lambda e^{-(s+\lambda)R_{TX}}} \\ &\approx \frac{\lambda(s + p/R_{TX})}{s^2 + s/R_{TX} + \lambda(1-p)/R_{TX}} \end{aligned}$$

[1] In the Appendix, we show the expected delay results of a *two-way* road section, where the vehicles in the opposite direction can assist the relay procedure.

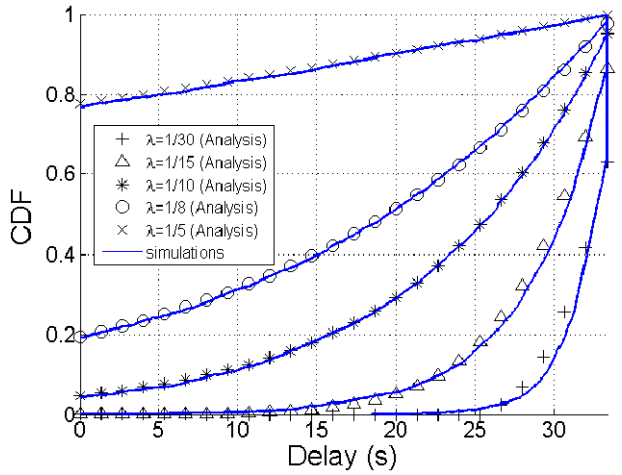

Fig. 3 Comparison of analytic and simulation results by showing the probability distribution of delay in a road section

where the last approximation is given by using $e^{-R_{TX}s} \approx 1/(1 + R_{TX}s)$. We then obtain the inverse Laplace transform of $H(s)$, which is $h(t)$, and finally derive $\Pr(C \le x)$ in (2) and (4).

$$h(t) = \begin{cases} \lambda \cdot e^{\frac{-t}{2R_{TX}}} \left[\cos\left(\frac{\sqrt{\alpha}}{2R_{TX}}t\right) + \frac{\lambda(2p-1)}{\sqrt{\alpha}} \sin\left(\frac{\sqrt{\alpha}}{2R_{TX}}t\right)\right] \\ \quad \text{if } \alpha \ge 0 \\ \lambda \cdot e^{\frac{-t}{2R_{TX}}} \left[\cosh\left(\frac{\sqrt{-\alpha}}{2R_{TX}}t\right) + \frac{\lambda(2p-1)}{\sqrt{-\alpha}} \sinh\left(\frac{\sqrt{-\alpha}}{2R_{TX}}t\right)\right] \\ \quad \text{if } \alpha < 0 \end{cases} \tag{6}$$

where $\alpha = 4\lambda(1-p)R_{TX} - 1$.

Given that the number of vehicles in a cluster is $n+1$, there will be n vehicles which receive the message via wireless transmissions and one store-and-carry within a road section, since a store-and-carry vehicle must carry the message to the next intersection. Therefore, the delay can be expressed as $D = (L - C)/v_{avg}$, where C is the advanced distance due to wireless transmissions, i.e., cluster length. From (4) and (6) the CDF of delay can be found as

$$\begin{aligned} F_D(y) &\equiv \Pr(D \le y) = \Pr(C \ge L - v_{avg}y) \\ &= 1 - \Pr(C < L - v_{avg}y) \end{aligned} \tag{7}$$

We plot the CDF of delay in Fig. 3 using the results of (7) and compare with the simulation results. The details of the simulation are presented in Sect. 6. We set $L = 500$ m, $R_{TX} = 30$ m, $v_{avg} = 15$ m/s. It is shown that the CDF of our analytic model and simulations match close together, validating that our analytic model is accurate. It is worth noting that in [6] and [14], the authors derived only the *expectation* of the cluster length while we derived the *probability distribution*. The probability distribution of delay (or cluster length) is necessary to assess the multi-copy diversity by acquiring the delay when multiple road paths choices are available as shown below.

Now consider the case when a vehicle located at an intersection can replicate the message to multiple road paths, i.e., multi-copy diversity is achievable. For example as shown in Fig. 1, vehicle A may take two road path choices to replicate the message, either the north way or the east way, so that the level of multi-copy diversity (k) is 2. By using (7), the CDF and PDF of delay with k road path choices can be expressed as follows

$$\begin{aligned} G_D(y,k) &\equiv \Pr(delay \le y | k \text{ diversity}) \\ &= 1 - \Pr(delay > y | k \text{ diversity}) \\ &= 1 - [1 - F_D(y)]^k \\ g_D(y,k) &\equiv \frac{d}{dy} G_D(y,k) = k \cdot f_D(y)[1 - F_D(y)]^{k-1} \end{aligned} \tag{8}$$

Finally, the expected delay with k roads path choices, i.e., multi-copy diversity of level k, can be shown as

$$\begin{aligned} \psi(k) &\equiv E[delay|k] = \int_0^{D_{MAX}} \{y \cdot g_D(y,k)\} dy \\ &\quad + (1 - G(D_{MAX}, k)) \cdot D_{MAX} \\ &= \int_0^{L/v_{avg}} \{ky \cdot f_D(y)[1 - F_D(y)]^{k-1}\} dy \\ &\quad + (1-p)^k \cdot L/v_{avg} \end{aligned} \tag{9}$$

where D_{MAX} is the maximum delay, which occurs when there are no wireless transmissions but only store-and-carry transmissions. Figure 4 presents the expected delay of a road section as the multi-copy diversity (k) increases as the vehicle density (λ) is varied. When λ is small (e.g., $\lambda = 1/30$), which means that the network is vastly disconnected, the expected delay decreases monotonically as the diversity (k) increases. Meanwhile, the expected delay decreases substantially with k when the λ is relatively larger (e.g., $\lambda = 1/10$). When λ is very large (e.g., $\lambda = 1/5$), meaning that the network is well connected, the expected delay approaches to 0 with k larger than 3, since we cannot achieve much gain through diversity. Note that epidemic routing [13] exploits maximum diversity by forwarding whenever possible. These results show that epidemic routing should achieve higher diversity gain over single-copy routing at intermediate densities (e.g., $\lambda = 1/10$ or $1/8$). This is in contrast to the expectation that epidemic routing achieves better performance at very low densities, in other words when the network is vastly disconnected (e.g., $\lambda = 1/30$). We present Table 1 for better understanding of the network connectivity degree at

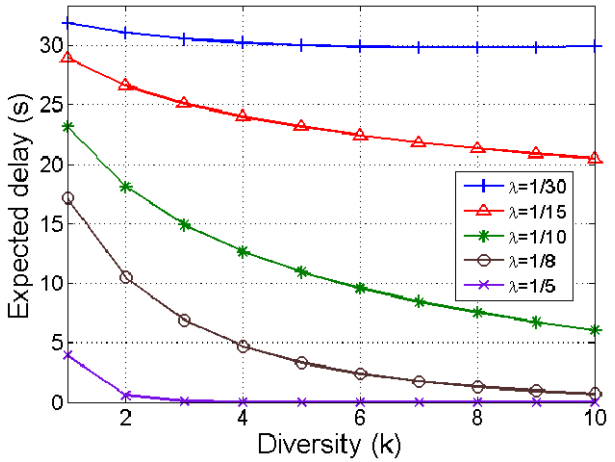

Fig. 4 Expected delay when k roads are available for routing (*multi-copy diversity* of level k) with variable vehicle density

Table 1 The probability of connectivity with a front vehicle and average cluster length on a 500 m road at various vehicular densities

Veh. density (λ, veh/m)	Prob. of connectivity with front veh.	Avg. cluster length on a 500 m road (m)
1/30	0.632	21.5
1/15	0.865	65.8
1/10	0.950	153.1
1/8	0.977	242.9
1/5	0.998	441.0

the given densities. In Sect. 4, we use this multi-copy diversity results to obtain an upper and lower bound of end-to-end routing delay.

3.3 Intersection analysis

In the previous subsection, we studied the first part of a vehicular network, a road section model. In this subsection we look into the other part of the vehicular network, the intersection model with traffic lights as illustrated in Fig. 5. We assume that vehicles travel forward which is either eastbound or northbound, and do not make turns. The traffic lights periodically change between red and green each with durations T_{red} and T_{green}. The probability that the current light is green (or red) is $P_{green} = 1 - P_{red}$ (or P_{red}) and the expected remaining time of the green (or red) light is $T_{green}/2$ (or $T_{red}/2$).

Let us assume that an eastbound vehicle A is holding the message at the intersection (shown in Fig. 5), where the message can go either (i) eastbound or (ii) northbound:

(i) Message is eastbound (goes to the same direction (forward) as current message holder, vehicle A)

When traffic light is red for eastbound traffic, vehicle A should wait until the traffic light turns to green. When traffic light is green, there is no waiting time. Therefore the expected waiting time when message is eastbound is,

$$E[D_{forward}] = P_{red} \times \frac{T_{red}}{2} + P_{green} \times 0 = \frac{P_{red} T_{red}}{2} \tag{10}$$

(ii) Message is northbound (makes a turn)

When traffic light is red, vehicle A should wait until a northbound vehicle appears. When traffic light is green, vehicle A forwards to a northbound vehicle that is waiting at the intersection. Therefore the expected waiting time when message is northbound is,

$$E[D_{turn}] = P_{red} \times \frac{1}{\lambda_t} + P_{green} \times \frac{T_{green}}{2} = \frac{1}{2\lambda_t} + \frac{P_{green} T_{TL}}{2} \tag{11}$$

where $\lambda_t = \lambda \cdot v_{avg}$ is the arrival rate of a north-bound vehicle.

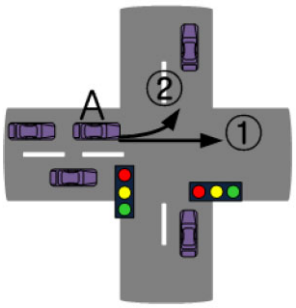

Fig. 5 Intersection model with traffic lights. The message, which is currently at vehicle A, can travel either (1) eastbound or (2) northbound

We use these results to study an upper and lower bound of end-to-end routing delay in Sect. 4.

4 An upper and lower-bound of end-to-end routing delay in sparse VANETs

In this section we derive an upper and lower-bound of end-to-end routing delay in sparse VANETs. Figure 1 shows an example of a source node A transmitting a message to destination B using multi-copy routing. Note that the message is forwarded only to the direction towards the destination B since the location of the destination is known. We denote the coordinates of the source node location as (0, 0) and that of the destination as (m, n) if the message has to travel through m horizontal and n vertical road sections to reach the destination. Therefore, in this example the destination coordinates are (3, 3). To derive the end-to-end routing performance, we divide the routing path into $(m + n)$ steps and obtain maximum multi-copy diversity at each step,

thus the minimum expected delay at each step. For example, in Fig. 1, there are 6 steps each shown as different shape arrow-lines and circled numbers. Each step consists of multiple available road paths so that the maximum multi-copy diversity level for each step is {2, 4, 6, 6, 4, 2}. Using (6), the minimum expected end-to-end delay of this example is expressed as follows:

$$E[D_{lower}] = \psi(2) + \psi(4) + \psi(6) + \psi + \psi(4) + \psi(2) + 6 \times E[D_{int\_lower}] \quad (12)$$

where $E[D_{int\_lower}]$ is the expected waiting time at the intersections derived from Sect. 3.3. We assume that the message makes a minimum number of turns (lowest delay), in this example one turn, so that $E[D_{int\_lower}] = E[D_{turn}] + 5 \cdot E[D_{forward}]$ in this case. We generalize the above equation for minimum expected delay from coordinates (0, 0) to (m, n) and express as follows:

$$E[D_{lower}] = \begin{cases} n \cdot \psi(1) + E[D_{int\_lower}], & m = 0 \\ (n-m) \cdot \psi(2m+1) +, & m \geq 1 \\ 2 \cdot \sum_{i=1}^{m} \psi(2i) + E[D_{int\_lower}] \end{cases} \quad (13)$$

where $m \leq n$. Notice that in case $m > n$ then we can switch m and n, since this gives the same result. We assume that the message makes a minimum number of turns for lower bound, so that $E[D_{int\_lower}] = E[D_{turn}] + (m + n - 1) \times E[D_{forward}]$. This formula shows a *lower-bound* of end-to-end routing delay which exploits the maximum multi-copy diversity, thus representing the minimum achievable delay by using epidemic routing with no resource constraints.

An upper-bound of end-to-end routing delay can be shown when there is no multi-copy diversity, which is the maximum delay of using single-copy routing. Therefore an upper-bound of end-to-end delay is expressed as follows:

$$E[D_{upper}] = (m + n) \times \psi(1) + E[D_{int\_upper}] \quad (14)$$

where $E[D_{int\_upper}]$ is again the expected waiting time at a intersections derived from Sect. 3.3. For upper bound, we assume that the message makes maximum number of turns, so that $E[D_{int\_upper}] = (m + n) \cdot E[D_{turn}]$ in this case.

We next study the numerical results, and compare with the simulations results that use epidemic routing. The specifications of the simulations are shown in Sect. 6 and Table 2. We set $L = 500$ m, $R_{TX} = 30$ m, $v_{avg} = 15$ m/s. Figure 6 plots the upper and lower-bound of end-to-end routing delay as a function of source-destination distance as the vehicle densities are varied. It is clear that the expected end-to-end delay increases as source-destination increases and as density decreases. The simulation results are well in-between the lower and upper-bound of the analytical results, showing that the analytical model is accurate.

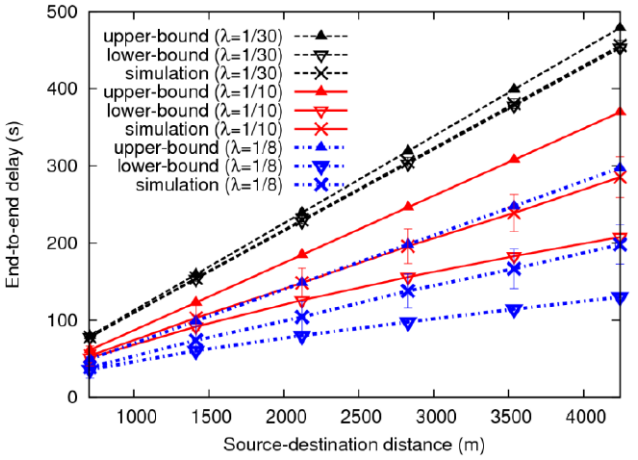

Fig. 6 Upper and lower-bound of end-to-end routing delay with increasing source-destination distance and variable vehicle density

As the source-destination distance increases, the number of available paths to the destination will also increase, thus a higher level of the multi-copy diversity gain, or lower end-to-end delay, can be expected. Notice again that the lower-bound of end-to-end delay is the case when maximum multi-copy diversity is achieved. When λ is very small (e.g., $\lambda = 1/30$), there is not much difference between the upper and lower-bound of expected end-to-end delay. Furthermore, the end-to-end delay linearly increases with source-destination distance. These results indicate that routing delay does not benefit from the increased multi-copy diversity, which are consistent with the results in Sect. 3.2 and Fig. 4. However, when λ is intermediate (e.g., $\lambda = 1/10$ or $1/8$), the difference between the upper and lower bound grows larger and also the slope of lower bound of delay decreases with source-destination distance, meaning that end-to-end delay decreases due to the multi-copy diversity gain. This result leads to the conclusion that multi-copy routing should be used in only partially-connected networks, since it does not benefit from the multi-copy diversity when the density is either too low or too high.

5 Adaptive multi-copy routing (AMR) protocol

In this section we present a heuristic Adaptive Multi-copy Routing protocol called AMR. In AMR, a vehicle at the intersection adaptively selects between single-copy and multi-copy routing by exploiting our analytical results which showed that the level of multi-copy diversity gain depends on the network connectivity. The intuition behind is that AMR will use multi-copy routing over single-copy routing only if the multi-copy gain is sufficiently high enough to overcome the overhead. In particular, if the end-to-end delay for using single-copy routing (upper-bound of multi-copy

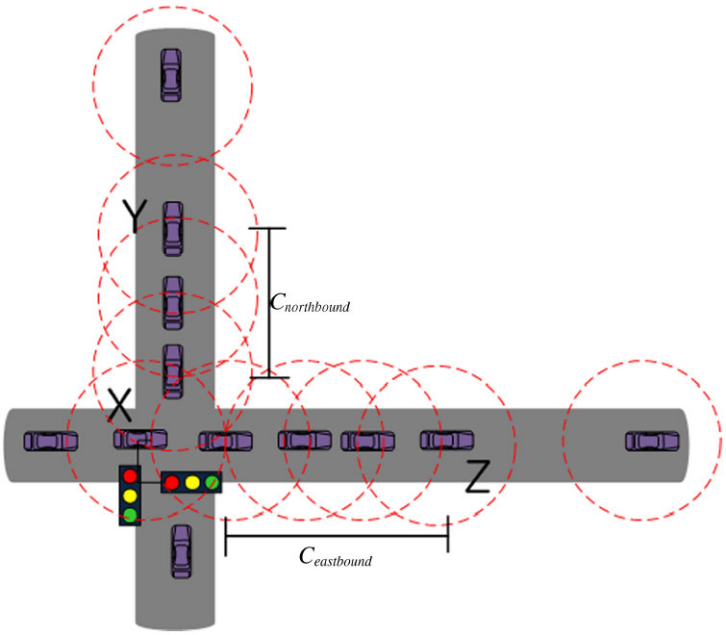

Fig. 7 Estimating the real-time local delay of the neighboring roads at an intersection. An intermediate node X, which is located at an intersection, sends probe packets to the northbound and eastbound road to estimate the real-time local delay. The last nodes of the cluster, which are Y and Z for northbound and eastbound roads, respectively, will send a reply packet notifying its current position, thus the cluster length

routing) is smaller than $(1+\alpha)\cdot ED_{opt}$, where α is a controlling parameter and ED_{opt} is the optimal (lower-bound) end-to-end delay, then single-copy routing is used, since the multi-copy diversity gain is not large enough. Otherwise, the multi-copy routing is used to exploit the multi-copy diversity gain. The parameter, α is a constraint that controls the tradeoff between end-to-end delay and overhead, which is a similar concept with the optimality control parameter used in [11]. We first describe the basic assumptions and ideas that AMR employs (Sect. 5.1) and then show the two basic stages of AMR: source node operation and intermediate node operation (Sect. 5.2).

5.1 Assumptions

A node in the vehicular network could be either a mobile vehicle or a fixed node (e.g., gas station sending/receiving advertisements or fixed access point at intersection collecting traffic information). We define a node located at the intersection as an *intermediate node*, since it decides which road section the message should be sent to. A node may identify itself as an intermediate node by using the location information and GPS map data, or by detecting methods presented in [8]. The nodes located on the road sections forward the message to the next intersection towards the path.

We make the following assumptions for practical considerations.

1. We assume that the road map data, the geographic location of the nodes itself and the destination are known to all the nodes in the network, due to GPS devices and location servers [17]. Therefore, the information can be utilized for location-aware routing [7].
2. We also assume that only the two following network parameters are available: the average vehicle density of the network and real-time *local delay*. The average vehicle density can be easily obtained by statistical data, as opposed to acquiring global network information at real-time, e.g., delay cost of every road section in the network [2, 10, 15]. The real-time local delay can be measured by the intermediate node sending a small probe packet to estimate the *cluster length* at a neighboring road. As soon as a vehicle in the message forwarding direction finds that the probe packet cannot be forwarded any further via wireless transmissions, it sends a reply packet to the originator of the probe informing its current location. For example as shown in Fig. 7, vehicle X, which is an intermediate node located at an intersection, sends probe packets to the northbound and eastbound roads to estimate the cluster length, therefore to measure the real-time local delay at each road. Then the last nodes of the clusters on each roads send a reply packet that reports the cluster lengths, e.g., vehicles Y and Z reports cluster lengths $C_{eastbound}$, and $C_{northbound}$, respectively. In result, node X acquires the real-time local delay at all the neighboring roads.

5.2 AMR details

The first stage that AMR takes is at the source node, which is formally described in Algorithm 1. First, the source node uses (13) and (14) to assess the end-to-end routing delay, since the destination location and the average vehicle density of the network is known (steps 1–2). If the multi-copy diversity gain is above α (step 3), then the source node uses

Algorithm 1 SrcNOp: Source Node Operation

1: Let the source node be *src* and the destination node be *dst*.
2: Define the lower and upper-bound of expected delay from node A to B as $ED_{lo}(A, B)$ and $ED_{up}(A, B)$, respectively.
3: Denote by $G_{multi\text{-}copy}$ the expected gain for using multi-copy routing over single-copy routing.

$$G_{multi\text{-}copy} = \frac{ED_{up}(src, dst) - ED_{lo}(src, dst)}{ED_{lo}(src, dst)}$$

4: **if** ($G_{multi\text{-}copy} \geq \alpha$) **then**
5: *src* uses *multi-copy routing*
6: **else**
7: *src* uses *greedy routing*
8: **end if**

multi-copy routing (steps 4–5). In multi-copy routing, the source node first copies the message to all available road sections towards the destination, then the intermediate nodes operates as explained below in the next stage of intermediate node operation. If the difference is below the threshold, *greedy routing* (also explained in the next stage) is used to reduce the routing overhead (steps 6–8).

The second stage is at the intermediate node, which is formally shown in Algorithm 2. First the intermediate node measures the real time local delays of all the potential next hop k roads $(R_1, \ldots, R_k)$ by using the method presented in Sect. 5.1 (steps 1–3). When *greedy routing* is initiated at the source node, then the intermediate node will use single-copy routing and forward the message only to the road which has lower local delay (steps 4–5). Since each intermediate node *greedily* selects the road based only on *local delay*, we define this scheme as *greedy routing*. Meanwhile, when *multi-copy routing* is initiated at the source node, the intermediate node decides whether to copy the message to one or all available roads (step 6). The intermediate node evaluates the expected delay to the destination by using both real-time local delay measurements and results from (13) and (14) (step 7). If the multi-copy diversity gain of taking all available roads over taking a single road is above β, then AMR exploits the multi-copy diversity and copies the message to all available roads (steps 8–9). In case the gain is below β, the intermediate node sends to the road with smaller expected delay, which is greed routing (steps 10–13). Notice that β is similar with the parameter α used in Algorithm 1, but β is used at the intermediate nodes only.

6 Simulations

In this section we validate our analytical model and also evaluate the performance of AMR via simulations. Note

Algorithm 2 IntNOp: Intermediate Node Operation

1: Let the intermediate node be *inter.* and the destination node be *dst.*
2: Define the lower and upper-bound of expected delay from node A to B as $ED_{lo}(A, B)$ and $ED_{up}(A, B)$, respectively. $D(R)$ represents the delay of passing a road R.
3: Node *inter.* has k choices of roads $(R_1, \ldots, R_k)$. If $k \geq 2$, then order roads $R_1, \ldots, R_k$ so that $D(R_i) \leq D(R_{i+1})$, where $i = 1, \ldots, k-1$. Define next hop-nodes (at intersection) by taking roads $R_1, \ldots, R_k$ as $N_1, \ldots, N_k$, *respectively*.
4: **if** (*greedy routing* is used at *src*) **then**
5: *inter.* forwards to road R_1 (node N_1)
6: **else if** (*multi-copy routing* is used at *src*) **then**
7: Denote by $G_{multi\text{-}copy}$ the expected multi-copy gain for copying the message to all available roads *vs.* to only R_1.

$$G_{multi\text{-}copy} = \frac{\{D(R_1) + ED_{lo}(N_1, dst)\} - ED_{lo}(int, dst)}{D(R_1) + ED_{lo}(N_1, dst)}$$

8: **if** ($G_{multi\text{-}copy} \geq \beta$) **then**
9: *inter.* copies message to roads $R_1, \ldots, R_k$ (nodes $N_1, \ldots, N_k$)
10: **else**
11: *inter.* forwards to only road R_1 (node N_1)
12: **end if**
13: **end if**

that in sparse networks, the message delivery delay is dominated by the message carrying delay (up to tens of seconds) rather than wireless transmission delay (up to a few milliseconds). Therefore, we developed a discrete event simulator that models the mobility of nodes but omits the wireless transmission delay, which is consistent with the previous work in [2, 6, 15]. We compare AMR with other previous routing protocols for sparse vehicular networks. The parameters used in our simulations are summarized in Table 2. We ran simulation tests to acquire the best constraint parameters for AMR, and hence set them as $\alpha = \beta = 0.1$. Recall that this means that AMR targets to achieve an end-to-end delay of a factor of 1.1 compared to the optimal end-to-end delay. Vehicles are randomly distributed on one-way roads with average density λ. We assume that the buffer size is not limited, which is quite general in vehicular networks since it can carry large storage devices [1].

We conducted two sets of simulations. We first investigate the enhanced performance of AMR compared with epidemic routing [13], Vehicle-Assisted Data Delivery (VADD) [15], and single-copy routing for variable vehicle densities. We then study the performance as the source-destination

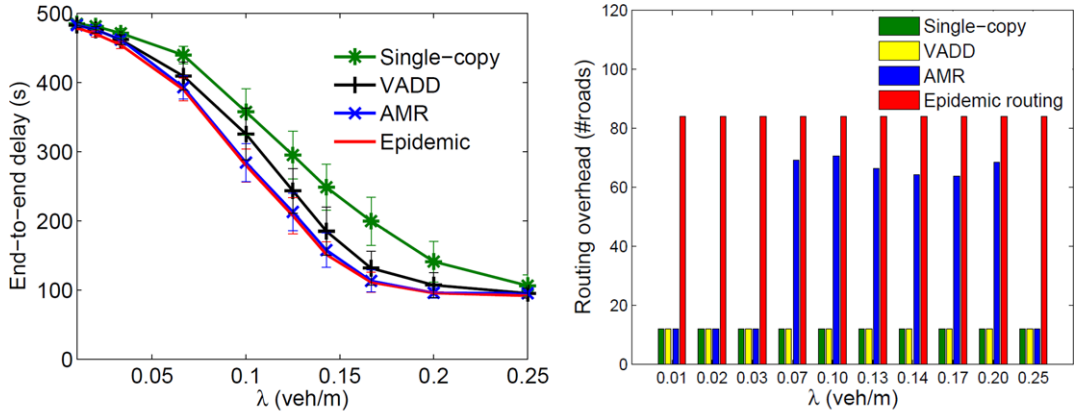

(a) End-to-end delay vs. vehicle density (b) Routing overhead vs. vehicle density

Fig. 8 Performance comparison of epidemic routing, AMR, VADD, and single-copy routing with variable vehicle density (source-destination distance = 4242 m)

Table 2 Simulation parameters

Parameter	Value
L (road length)	500 m
v_{avg} (vehicle speed)	15 m/s
Transmission range (R_{TX})	30 m
Green light period (T_{green})	30 s
Red light period (T_{red})	30 s
α, β	0.1

distance is increased to compare AMR's performance with other protocols. We use two performance criteria in the simulations: end-to-end delay and routing overhead. The end-to-end delay is the message delivery delay, dominated by store-and-carry delay, from source to destination. The routing overhead is measured by the number of roads that participate in the routing process. This criterion is similar to the term *infected nodes* used in DTNs, e.g., *epidemic routing* [13, 16], but we use *roads* instead of *nodes*. We averaged each of the simulation results for 20 runs.

Figure 8(a) shows the end-to-end delay of AMR with variable vehicle densities, and compare with other protocols. We fix the source-destination distance to 4242 m (6 by 6 blocks), and gradually increased the average vehicle density from 1/100 to 1/4 veh/m (x-axis). AMR consistently outperforms both single-copy routing by up to 43% and 18% in average, and outperforms VADD by up to 18% and 13% in average, regardless of the vehicle density, due to multi-copy diversity. In the mean time, it closely approaches the delay performance of epidemic routing. Figure 8(b) depicts the routing overhead as the density increases. When the density is either very small, e.g., $\lambda = 1/100$, or very large, e.g., $\lambda = 1/4$, AMR and single-copy routing shows similar routing overhead while achieving lower end-to-end delay, since AMR adaptively employs *greedy routing* when the multi-copy diversity is not large enough. AMR applies *multi-copy routing* when network connectivity is partial, e.g., $\lambda = 1/10$, and achieves the multi-copy diversity gain close to epidemic routing with decreased routing overhead by up to 86% and 46% in average. VADD achieves smaller routing overhead by sacrificing the end-to-end delay performance.

Figure 9(a) plots the end-to-end delay of the four routing protocols when source-destination distance is varied with fixed average vehicle density $\lambda = 1/8$. The source-destination distance is increased from 707 m (1 by 1 block) to 4949 m (7 by 7 blocks). Similar to the results in Fig. 8, AMR consistently outperforms single-copy routing by up to 32% and 25% in average, and outperforms VADD by up to 19% and 13% in average. Meanwhile, it closely approaches the performance epidemic routing in terms of end-to-end delay. As shown in Fig. 9(b), AMR reduces routing overhead by up to 21% and 20% in average compared to epidemic routing.

7 Conclusion

In this paper, we developed an analytical framework to evaluate the multi-copy diversity effect on the performance of routing in sparse vehicular ad hoc networks. In particular, we derived the probability distribution of delay when it is possible to replicate the message to multiple roads at the intersection, consequently yielding an upper-bound and lower-bound of end-to-end delay of multi-copy routing. In contrast to the expectations, higher multi-copy diversity gain is achieved when the network is partially connected as opposed to the cases when the network is either connected very well or mostly disconnected. Simulation results validated that our analytical model is very accurate.

Furthermore, we proposed AMR, an Adaptive Multi-copy Routing protocol. AMR exploits our analytic results

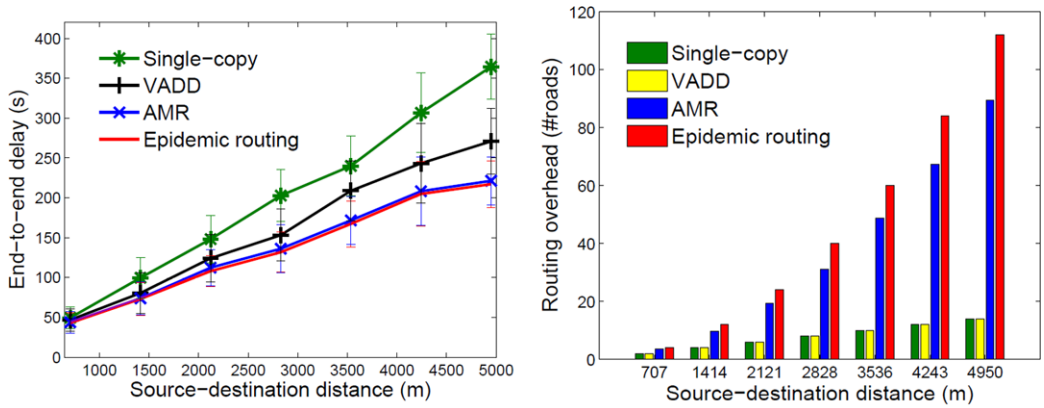

(a) End-to-end delay vs. source-destination distance

(b) Routing overhead vs. source-destination distance

Fig. 9 Routing overhead comparison of epidemic routing, AMR, VADD and single-copy routing with variable source-destination distance ($\lambda = 1/8$ veh/m)

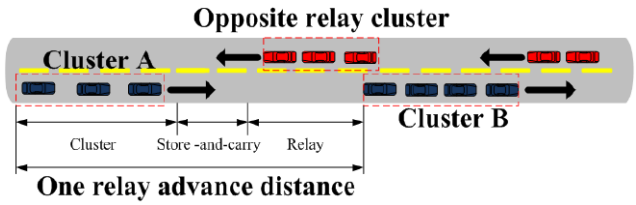

Fig. 10 Two-way road section model. Cluster A forwards the message to cluster B via an opposite relay cluster at the opposite lane. *One relay advance* distance is defined as the sum of cluster length at current lane (cluster A), store-and-carry forwarding distance, and a relay at the opposite lane

and adaptively limits the routing overhead by using local delay measurements only. Simulation results showed that AMR achieves end-to-end delay comparable to that of epidemic routing while significantly reducing the routing overhead by up to 86%.

Acknowledgements This work was supported in part by the KOSEF (R01-2007-000-20154-0) and by the MKE (The Ministry of Knowledge Economy), Korea, under the ITRC (Information Technology Research Center) support program supervised by the NIPA (National IT Industry Promotion Agency) (NIPA-2010-(C1090-1011-0004)), and by the National Research Foundation of Korea Grant funded by the Korean Government (NRF-2009-352-D00261).

Appendix: Two-way road section analysis

In this section, we extend the one-way road section model presented in Sect. 3.2 by studying the expected delay of a two-way road section. The main difference is that the vehicles on the opposite lane may relay the message to the forward cluster. For example in Fig. 10, the message in cluster A may be relayed to cluster B via a cluster at the opposite lane, which we call *opposite relay cluster*. Notice that a opposite relay cluster may relay the message only through direct wireless transmissions, not store-and-carry, since the vehicles at the opposite lane travel at opposite directions, and hence cannot carry the message to the desired direction (note that in [14], the authors assume that the message can be store-and-carried only by the vehicles in the opposite direction, which is different from our assumptions). Therefore the opposite relay cluster has to be within the transmission range of both the current cluster and the forward cluster at the time of relay. For example in Fig. 10, for the opposite relay cluster to be able to relay the message from cluster A to cluster B, it has to be within transmission range of both clusters A and B at the time of relay.

We start by describing the definition of the term *one relay advance* distance, which represents the total message advance distance when a opposite relay cluster relays a message from the current cluster to the forward cluster. It is defined as the sum of an advance distance due to wireless transmissions within a cluster at the current lane (cluster A), a store-and-carry distance until it meets a relay cluster at the opposite lane, and a relay transmission distance via a opposite relay cluster (see Fig. 10). The expectation of *one relay advance* distance can be expressed as follows:

$$E[\text{advance}] = E[\text{cluster}] + E[\text{store-and-carry}] + E[\text{relay}] \quad \text{(A.1)}$$

The first and third term in the right part of (A.1) can be obtained as follows. $E[\text{cluster}]$ is the expected cluster length

which can be obtained directly from (4) so that $E[\text{cluster}] = p/((1-p)\lambda) - R_{TX}$. $E[\text{relay}]$ is same as the expected inter-cluster distance of the current lane. Therefore, the CDF of inter-cluster distance (X_{INTER}) is

$$F(X_{INTER}) \equiv \Pr(X_{INTER} \le x | X_{INTER} > R_{TX}) = \frac{\int_{R_{TX}}^{x} \lambda e^{-\lambda t} dt}{e^{-\lambda R_{TX}}} = 1 - e^{-\lambda(x - R_{TX})} \quad \text{(A.2)}$$

Therefore, the expected inter-cluster distance is $E[X_{INTER}] = 1/\lambda + R_{TX} = E[\text{relay}]$, which represents the last term of (A.1).

To acquire the store-and-carry distance ($E[\text{store-and-carry}]$) in (A.1), we must first derive how many vehicles cluster A (Fig. 10) should pass by before it finally meets a relay cluster that can actually relay the message to the cluster in front (cluster B in Fig. 10). Recall that for the relay cluster to be able to relay, it must be within transmission range of both the clusters A and B at the instant of relay transmission. From (A.2), for the opposite relay cluster to be able to relay the message from clusters A to relay cluster and then to B, the next condition must hold

$$\Pr(X_{INTER} \le C + 2R_{TX}) \approx F_{INTER}(E[C] + 2R_{TX}) = 1 - e^{-\lambda(R_{TX}^{+E[C]})} \equiv P_{relay} \quad \text{(A.3)}$$

where X_{INTER} is a random variable for inter-cluster distance, $E[C]$ is the expected cluster length, and P_{relay} is the probability that the vehicle at the opposite lane can relay to the forward cluster. Note that this is an approximation, since we used two expectation terms in the probability condition (A similar approach was used in [14]). The expected number of pass-by vehicles at the opposite lane before meeting the actual relay cluster is the mean of geometric distribution by using (A.3),

$$E[N_{relay}] = \sum_{n=1}^{\infty} n \cdot P_{relay}(1 - P_{relay})^{n-1} = \frac{1}{P_{relay}} \quad \text{(A.4)}$$

Next we describe the distance to the opposite relay cluster, i.e., store-and-carry distance. The expected distance to a vehicle at the opposite lane is $E[X_{opposite}] = 1/\lambda_o$, where λ_o is the vehicle density at the opposite lane. Therefore, the expected distance to the relay-capable vehicle is given as follows:

$$E[X_{relay}] = E[X_{opposite}] \times E[N_{relay}] = \frac{1}{\lambda_o P_{relay}} = E[\text{store-and-carry}] \quad \text{(A.5)}$$

Through (A.2)∼(A.5), equation (A.1) can be rewritten as follows:

$$E[\text{advance}] = E[\text{cluster}] + E[X_{relay}] + E[X_{INTER}] = \frac{\lambda(1-p) + \lambda_o P_{relay}}{\lambda\lambda_o(1-p)P_{relay}} \quad \text{(A.6)}$$

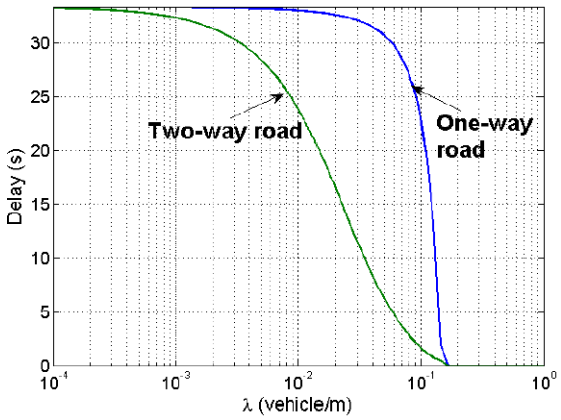

Fig. 11 Expected delay of a one-way and two-way road section

We now explain the expected delay during *one relay advance*. Since we assume that wireless transmission delay ≈ 0, by using (A.5), the expected delay of *one relay advance* is,

$$E[D_{advance}] = E[X_{relay}]/v_{avg} = \frac{1}{\lambda_o v_{avg} P_{relay}} \quad \text{(A.7)}$$

Finally, the expected delay of a message in a two-way road of length L is

$$E[D_{two\text{-}way}] = E[D_{advance}] \times L/E[\text{advance}] = \frac{L}{\left(\frac{\lambda_o P_{relay}}{\lambda(1-p)} + 1\right) v_{avg}} \quad \text{(A.8)}$$

Figure 11 depicts the expected delay of a one-way versus a two-way road section as the vehicle density in the network varies. For simplicity, we give the distribution of vehicles at the opposite lane same as that of the current lane. As we expect, the delay performance of a two-way road section consistently outperforms that of a one-way road section by up to 94% (when $\lambda = 1/8$), since it benefits from the relay cluster at the opposite lane. In this paper, we use the results of a one-way road section (Sect. 3.2), although we have derived the expected delay of a two-way road section, since we require the probability distribution of delay rather than just the expected value to assess the multi-copy diversity.

References

1. Burgess, J., Gallagher, B., Jensen, D., & Levine, B. (2006). MaxProp: Routing for vehicle-based disruption-tolerant networks. In *IEEE Infocom'06*, Barcelona, Spain.
2. Ding, Y., Wang, C., & Xiao, L. (2007). A static-node assisted adaptive routing protocol in vehicular networks. In *ACM VANET'07*, Montreal, Canada.

3. Fiore, M., & Harri, J. (2008). The networking shape of vehicular mobility. In *ACM Mobihoc'08*, Hong Kong SAR, China.
4. Fiore, M., Harri, J., Filali, F., & Bonnet, C. (2007). Vehicular mobility simulation for VANETs. In *ANSS'07*, Ottawa, Canada.
5. Huang, H., Luo, P., Li, M., Shu, W., & Wu, M. (2007). Performance evaluation of SUVnet with real-time traffic data. *IEEE Transactions on Vehicular Technology*, *56*(6), 3381–3396.
6. Jeong, J., Guo, S., Gu, Y., He, T., & Du, D. (2009). TBD: Trajectory-based data forwarding for light-traffic vehicular networks. In *IEEE ICDCS'09*, Montreal, Quebec, Canada.
7. Karp, B., & Kung, H. (2000). GPSR: greedy perimeter stateless routing for wireless networks. In *ACM Mobicom'00*, Boston, Massachusetts.
8. Lochert, C., Mauve, M., Fuessler, H., & Hartenstein, H. (2005). Geographic routing in city scenarios. *ACM SIGMOBILE Mobile Computing and Communications Review*, *9*(1), 69–72.
9. Mohimani, G., Ashtiani, F., Javanmard, A., & Hamdi, M. (2009). Mobility modeling, spatial traffic distribution, and probability of Connectivity for Sparse and Dense Vehicular Ad Hoc Networks. *IEEE Transactions on Vehicular Technology*, *58*(4), 1998–2007.
10. Skordylis, A., & Trigoni, N. (2008). Delay-bounded routing in vehicular ad hoc networks. In *ACM Mobihoc'08*, Hong Kong SAR, China.
11. Spyropoulos, T., Psounis, K., & Raghavendra, C. (2008). Efficient routing in intermittently connected mobile networks: The multiple-copy case. *ACM/IEEE Transactions on Networking*, *16*(1), 77–90.
12. Tonguz, O., Viriyasitavat, W., & Bai, F. (2009). Modeling urban traffic: A cellular automata approach. *IEEE Communications Magazine*, *47*(5), 142–150.
13. Vahdat, A., & Becker, D. (2000). Epidemic routing for partially connected ad hoc networks. *Technical report CS-2000*, Duke University.
14. Wisitpongphan, N., Bai, F., Mudalige, P., Sadekar, V., & Tonguz, O. (2007). Routing in sparse vehicular ad hoc wireless networks. *IEEE Journal of Selected Areas in Communication*, *25*(8), 1538–1556.
15. Xhao, J., & Cao, G. (2006). VADD: Vehicle-assisted data delivery in vehicular ad hoc networks. In *IEEE Infocom'06*, Barcelona, Spain.
16. Zhang, X., Neglia, G., Kurose, J., & Towsley, D. (2007). Performance modeling of epidemic routing. *Computer Networks*, *51*(10), 2859–2891.
17. Zhu, H., Zhu, Y., Li, M., & Ni, L. M. (2008). HERO: Online real-time vehicle tracking in Shanghai. In *IEEE Infocom'08*, Phoenix, Arizona.

Joon Yoo received his B.S. in Mechanical Engineering from Korea Advanced Institute of Science and Technology (KAIST), and Ph.D in Computer Science and Engineering from Seoul National University in 1997 and 2009, respectively. He worked as a research professor at University of Seoul in 2009. From 2009 to 2010, he worked as a post-doctoral researcher at the University of California, Los Angeles. Since December 2010, he has been with Alcatel-Lucent Bell Labs Seoul as a Member of Technical Staff. His research interests include vehicular ad hoc networks, mesh networks, cognitive radio and IEEE 802.11 and 802.16.

Sunwoong Choi received the B.S. and M.S. degrees in computer science and the Ph.D. degree in electrical engineering and computer science from Seoul National University in 1998, 2000, and 2005, respectively. From 2005 to 2007, he was with Samsung Electronics Company, Ltd., Kyungki-do, Korea, where he contributed to the design and development of Mobile WiMAX system. Since February 2007, he has been with the School of Electrical Engineering, Kookmin University, Seoul, where he is currently an Assistant Professor. His research interests include wireless networks, resource management, and performance evaluation.

Chong-kwon Kim received the B.S. degree in industrial engineering from Seoul National University, the M.S. degree in operations research from Georgia Institute of Technology, and the Ph.D. degree in Computer Science from University of Illinois at Urbana-Champaign in 1981, 1982, and 1987, respectively. In 1987, he joined Bellcore as a Member of Technical Staff and worked on Broadband ISDN and ATM. Since 1991, he has been with Seoul National University as a Professor in the School of Computer Science and Engineering. His research interests include wireless and mobile networking, high speed network control, distributed processing, and performance evaluation.